

A FAST ITERATIVE ALGORITHM FOR NEAR-DIAGONAL EIGENVALUE PROBLEMS*

MASEIM KENMOE[†], RONALD KRIEMANN[‡], MATTEO SMERLAK[‡], AND ANTON S. ZADORIN[‡]

Abstract. We introduce a novel iterative eigenvalue algorithm for near-diagonal matrices termed *iterative perturbative theory* (IPT). Built upon a “perturbative” partitioning of the matrix into diagonal and off-diagonal parts, IPT has the complexity of one matrix-vector (when one eigenpair is requested) or one matrix-matrix multiplication (when all eigenpairs are requested) per iteration. Thanks to the high parallelism of these basic linear algebra operations, we obtain excellent performance on multi-core processors and GPUs, with large speed-ups over standard methods (up to $\sim 50\times$ with respect to LAPACK and ARPACK, $\sim 5\times$ with respect to Davidson). When off-diagonal elements are comparable to eigengaps, IPT diverges like the quadratic map outside the Mandelbrot set; for such general matrices IPT can nevertheless be used to refine low-precision eigenvectors obtained by other methods. We give sufficient conditions for linear convergence and demonstrate performance on dense and sparse test matrices.

Key words. eigenvalue algorithm, perturbation theory, iterative refinement, dynamical systems

AMS subject classifications. 65F15

1. Introduction. Computing the eigenvalues and eigenvectors of a matrix that is already close to being diagonal (or diagonalizable in a known basis) is a classic problem throughout science. *Ab initio* studies of electronic and nuclear structures, for instance, often involve Hamiltonian operators expressed in bases that nearly diagonalize them, *e.g.* for self-consistent field or configuration interaction calculations [1]. In classical electromagnetism, perturbative problems arise when the solution to a slightly deformed problem are sought, for instance when boundary conditions are shifted or optical properties are varied [2]. In mechanical engineering, one often wants to know the effect of slight deformations of stiffness or density on spectra, as in Rayleigh’s pioneering analysis of vibrating strings [3]. More generally, we might know approximate eigenpairs through some method, and the problem is to refine them to a given precision.

Eigenvalue perturbation theory provides estimates and bounds for the variation of eigenpairs with respect to perturbations of the matrix [4]. Here our aim is, instead, to compute these eigenpairs exactly (up to numerical error), *i.e.* we are interested in eigenvalue algorithms for perturbative problems. In the symmetric case, algorithms that take advantage of near diagonality are available. Thus, when just a few extremal eigenpairs are desired, Davidson-type subspace iteration methods [5] can be efficient, with large speed-ups over Lanczos [6]. To obtain the complete set of eigenvectors of near-diagonal symmetric matrices, Jacobi’s algorithm may be advised: its local quadratic convergence and parallelizability imply that converged eigenvectors can sometimes be obtained in a fraction of the time required for tri-diagonalization. This is especially true on modern graphical processing units (GPUs), whose massive paral-

*Submitted to the editors in Dec. 2020.

Funding: Funding for this work was provided by the Alexander von Humboldt Foundation in the framework of the Sofja Kovalevskaja Award endowed by the German Federal Ministry of Education and Research.

[†]University of Dschang, Cameroon, and Max Planck Institute for the Mathematical Sciences, Leipzig, Germany

[‡]Max Planck Institute for the Mathematical Sciences, Leipzig, Germany

leism allow for extremely high flop rates that can sometimes offset the unfavourable complexity of Jacobi's algorithm [7].

Here we introduce a novel iterative algorithm for the computation of one or all eigenpairs of a near-diagonal matrix. While more restricted in its applicability than Davidson- or Jacobi-like methods, its performance is higher. This follows from our algorithm's simple linear-algebraic structure: each iteration consists of just one matrix-vector multiplication (for one eigenpair) or one matrix-matrix multiplication (for all eigenpairs). These operations are highly optimized in the Basic Linear Algebra Subprograms (BLAS Level 2 and 3 respectively), resulting in comparatively lower execution times. Moreover, since matrix-matrix multiplication has sub-cubic theoretical complexity $\mathcal{O}(N^{2.376})$, so does our algorithm, in contrast with classical algorithms which are $\mathcal{O}(N^3)$.

Iterative perturbation theory (IPT) was inspired by the Rayleigh-Schrödinger (RS) perturbative expansion familiar from textbook quantum mechanics [8]. (The relationship between the two methods, together with applications to physical and chemical examples, will be discussed in a companion paper [9].) Its structure, however, is different: instead of seeking the perturbed eigenvectors as power series in the perturbation, we compute them iteratively, as fixed points of a quadratic equation. One consequence of this difference is that, unlike Rayleigh-Schrödinger expansions [10], the domain of convergence of our method as a scalar perturbation parameter is varied is not restricted to a disk in the complex plane bounded by exceptional points (values of the parameter such that the matrix is defective); instead, IPT behaves for large perturbation like the logistic map, i.e. it follows the period-doubling route to chaos.

Our presentation starts with a reformulation of the eigenvalue equation as a fixed point equation for a quadratic map in complex projective space (section 2). We then establish a sufficient condition for fixed point iteration to converge and illustrate its divergence for larger perturbations with a simple two-dimensional example (section 3). Next, we consider the computational efficiency of our method on multi-CPU and GPU architectures using random test matrices (section 4). We then discuss one possible application of our algorithm as a refinement method for eigenvectors (section 5). We conclude with some possible directions for future work.

2. Eigenvectors as fixed points. Let us begin with the observation that, being defined up to a multiplicative constant, the eigenvectors of a matrix $M = (M_{mn})_{1 \leq n, m \leq N}$ are naturally viewed as elements of the complex projective space \mathbb{CP}^{N-1} . Let $[z_1 : \dots : z_N]$ denote the homogeneous coordinates of $z \in \mathbb{CP}^{N-1}$. Fix an index $1 \leq n \leq N$, and consider an eigenvector z of M such that $z_n \neq 0$. From the eigenvalue equation $Mz = \varepsilon z$ we can extract its eigenvalue as $\varepsilon = (Mz)_n / z_n$; inserting this back into $Mz = \varepsilon z$ shows that z is a projective root of the system of $N - 1$ homogeneous quadratic equations

$$(2.1) \quad (Mz)_m z_n = (Mz)_n z_m \quad \text{for } m \neq n.$$

Denoting V_n the projective variety defined by these equations and U_n the affine chart in which the n -th homogeneous coordinate is nonzero, the set of eigenvectors of M can therefore be identified with the affine variety $\cup_n (V_n \cap U_n)$ (Appendix A). Since eigenvectors generically have non-zero coordinates in all directions, each component $V_n \cap U_n$ typically contains the complete set of eigenvectors.

Algorithm 2.1 One eigenvector of a near-diagonal matrix M

- 1: Choose a partition $M = D + \Delta$ with D diagonal
 - 2: Compute $\theta_n \leftarrow ((D_{nn} - D_{mm})^{-1})_m$ and set $\theta_{nn} = 0$
 - 3: Initialize $z \leftarrow e_n$
 - 4: **while** z not converged **do**
 - 5: $z \leftarrow F_n(A)$ with F defined by (2.2)
 - 6: **end while**
 - 7: Return eigenvector z
 - 8: Return eigenvalue $\varepsilon_n = D_{nn} + (\Delta z)_n$
-

We now further assume a perturbative partitioning

$$M = D + \Delta,$$

where the diagonal part D consists of unperturbed eigenvalues ϵ_n . In practice D can be taken as the diagonal elements of M , although different partitionings can sometimes be more appropriate [11]. Provided the ϵ_n 's are all simple (non-degenerate), we can rewrite the polynomial system (2.1) as

$$z_n z_m = \theta_{mn} (z_n (\Delta z)_m - z_m (\Delta z)_n) \text{ for } m \neq n,$$

where $\theta_{mn} \equiv (\epsilon_m - \epsilon_n)^{-1}$ and we set $\theta_{nn} = 0$. Within the chart U_n containing the basis vector $e_n = (\delta_{mn})_{1 \leq m \leq N}$ we are free to set $z_n = 1$, resulting in the fixed point equation $z = F_n(z)$ with $F_n : U_n \rightarrow U_n$ is the map

$$(2.2) \quad F_n(z) = e_n + \theta_n \circ ((\Delta z)_n z - \Delta z).$$

Here we denoted $\theta_n = (\theta_{mn})_{1 \leq m \leq N}$ and \circ denotes the element-wise product of vectors. To obtain the eigenvector of M closest to the basis vector e_n , we can solve (2.2) by fixed-point iteration; this is the basic idea of our method. As noted, each iteration of F_n consists of a single multiplication of the present vector by the perturbation Δ , followed by element-wise multiplication by the vector θ_n .

The same iterative technique can be used to compute all eigenvectors of M in parallel. For this it suffices to bundle all N candidate eigenvectors for each n into a matrix A and apply the map F_n to the n -th column of A . This corresponds to the matrix map

$$(2.3) \quad F(A) \equiv I + \theta \circ (A \mathcal{D}(\Delta A) - \Delta A),$$

where \circ denotes the Hadamard (element-wise) product of matrices and $\mathcal{D}(M)$ is the diagonal matrix built with the diagonal elements of M . Starting from $A^{(0)} = I$, we obtain a sequence of matrices $A^{(k)} = F(A^{(k-1)})$ whose limit as $k \rightarrow \infty$ is the full set of eigenvectors. We call this approach *iterative perturbation theory* (IPT).

3. Convergence and divergence. In this section we look at the convergence of fixed-point iteration for the map (2.3). In a nutshell, the off-diagonal elements Δ must be small compared to the diagonal gaps $\epsilon_n - \epsilon_m$, a typical condition for eigenvector perturbation theory [10].

Algorithm 2.2 Full eigendecomposition of a near-diagonal matrix M

-
- 1: Choose a partition $M = D + \Delta$ with D diagonal
 - 2: Compute $\theta \leftarrow ((D_{nn} - D_{mm})^{-1})_{n \neq m}$ and set $\theta_{nn} = 0$
 - 3: Initialize $A \leftarrow I$
 - 4: **while** A not converged **do**
 - 5: $A \leftarrow F(A)$ with F defined by (2.3)
 - 6: **end while**
 - 7: Return eigenmatrix A
 - 8: Return eigenvalues $E = D + \mathcal{D}(\Delta A)$
-

3.1. A sufficient condition for convergence. Linear convergence of $A^{(k)}$ for small perturbations Δ follows from a simple contraction argument. Let $\|\cdot\|$ denote the spectral norm of matrices (the largest singular value), which is sub-multiplicative with respect to both the matrix and Hadamard products [12]. First, $\|F(A) - I\| \leq \|\theta\| \|\Delta\| (\|A\| + \|A\|^2)$ implies that F maps a closed ball $B_r(I)$ of radius r centered on I onto itself whenever $\|\theta\| \|\Delta\| \leq r / [(1+r)(2+r)]$. Next, from (2.3) we have

$$\|F(A) - F(B)\| \leq \|\theta\| \|\Delta\| (1 + \|A + B\|) \|A - B\|.$$

Hence, F is contracting in $B_r(I)$ provided $\|\theta\| \|\Delta\| < 1 / [1 + 2(1+r)]$. Under these conditions the Banach fixed-point theorem implies that $A^{(k)} = F^k(I)$ converges exponentially to a unique fixed point A^* within this ball as $k \rightarrow \infty$. Choosing the optimal radius

$$\operatorname{argmax}_{r>0} \min \left(\frac{r}{(1+r)(2+r)}, \frac{1}{1+2(1+r)} \right) = \sqrt{2},$$

we see that $\|\Delta\| < (3 - 2\sqrt{2}) \|\theta\|^{-1} \approx 0.17 \|\theta\|^{-1}$ guarantees convergence to the fixed point A^* . We show in Appendix B that the columns of A^* indeed form an eigenbasis of M .

3.2. Contrast with RS perturbation theory. It is interesting to contrast the present iterative method with conventional RS perturbation theory, where the eigenvectors of a parametric matrix $M = D + \lambda \Delta$ are sought as power series in λ , viz. $z = \sum_{\ell} z^{(\ell)} \lambda^{\ell}$. Identifying the terms of the same order in λ in the eigenvalue equation, one obtains for the matrix of eigenvectors at order k $A_{\text{RS}}^{(k)} = \sum_{\ell=0}^k a^{(\ell)} \lambda^{\ell}$ in which the matrix coefficients $a^{(\ell)}$ are obtained from $a^{(0)} = I$ via the recursion (Appendix C)

$$(3.1) \quad a^{(\ell)} = \theta \circ \left(\sum_{s=0}^{\ell-1} a^{(\ell-1-s)} \mathcal{D}(\Delta a^{(s)}) - \Delta a^{(\ell-1)} \right).$$

The iterative scheme $A^{(k)}$ completely contains this RS series, in the sense that $A^{(k)} = A_{\text{RS}}^{(k)} + \mathcal{O}(\lambda^{k+1})$; this can be seen by induction (Appendix D). In other words, we can recover the usual perturbative expansion of A to order k by iterating k times the map F and dropping all terms $\mathcal{O}(\lambda^{k+1})$. Moreover, the parameter whose smallness determines the convergence of the RS series is the product of the perturbation magnitude λ with the inverse diagonal gaps θ [10], just as it determines the contraction property of F .

But IPT also differs from the RS series in two key ways. First, the complexity of each iteration is constant (essentially just one matrix product with Δ), whereas computing the RS coefficients $a^{(\ell)}$ involves the sum of increasingly many matrix products.

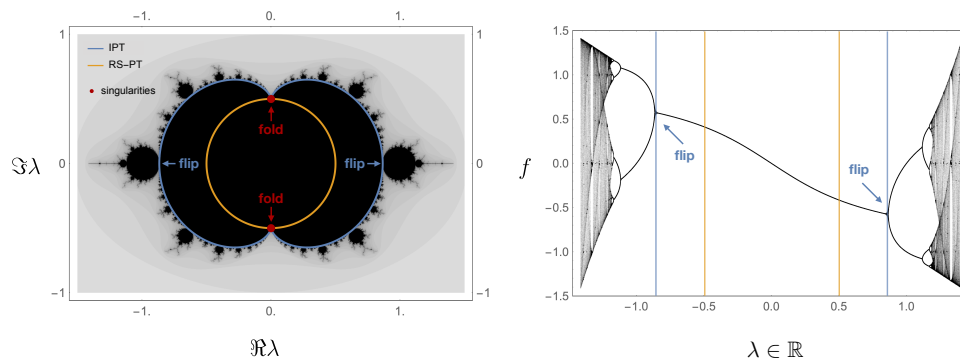


FIG. 1. *Convergence of IPT in the two-dimensional example (3.2). Left: In the complex λ -plane, RS perturbation theory (RS-PT) converges inside a circle of radius $1/2$ (orange line) bounded by the exceptional points $\pm i/2$ where eigenvalues have branch-point singularities and M is not diagonalizable. Dynamical perturbation theory (IPT) converges inside the domain bounded by the blue cardioid, which is larger—especially along the real axis, where there is no singularity. Outside this domain, the map can converge to a periodic cycle, be chaotic or diverge to infinity, following flip bifurcations (along the real axis) and fold bifurcations (at the singularities). The domain where the map remains bounded (black area) is a conformal transformation of the Mandelbrot set. Right: The bifurcation diagram for the quadratic map f along the real λ -axis illustrates the period-doubling route to chaos as λ increases away from 0 (in absolute value). Orange and left vertical lines indicate the boundary of the convergence domains of RS-PT and IPT respectively.*

Second, not being defined as a power series, the convergence of $A^{(k)}$ when $k \rightarrow \infty$ is not *a priori* restricted to a disk in the complex λ -plane. Together, these two differences suggest that IPT has the potential to converge faster, and in a larger domain, than RS perturbation theory. This is what we now examine, starting from an elementary but explicit example.

3.3. An explicit 2×2 example. To build intuition, let us consider the parametric matrix

$$(3.2) \quad M = \begin{pmatrix} 0 & \lambda \\ \lambda & 1 \end{pmatrix}.$$

This matrix has eigenvalues $\varepsilon_{\pm} = (1 \pm \sqrt{1 + 4\lambda^2})/2$, both of which are analytic inside the disk $|\lambda| < 1/2$ but have branch-point singularities at $\lambda = \pm i/2$. (These singularities are in fact exceptional points, *i.e.* M is not diagonalizable for these values.) Because the RS series is a power series, these imaginary points contaminate its convergence also on the real axis, where no singularity exists: A_{RS} diverges for any value of λ outside the disk of radius $1/2$, and in particular for real $\lambda > 1/2$.

Considering instead our iterative scheme, one easily computes

$$A^{(k)} = \begin{pmatrix} 1 & f^k(0) \\ -f^k(0) & 1 \end{pmatrix},$$

where $f(x) = \lambda(x^2 - 1)$ and the superscripts indicate k -fold iterates. This one-dimensional map has two fixed points at $x_{\pm}^* = \varepsilon_{\pm}/\lambda$. Of these two fixed points x_+^* is always unstable, while x_-^* is stable for $\lambda \in (-\sqrt{3}/2, \sqrt{3}/2)$ and loses its stability at $\lambda = \pm\sqrt{3}/2$ in a flip bifurcation. At yet larger values of λ , the iterated map

f^k —hence the fixed-point iterations $A^{(k)}$ —follows the period-doubling route to chaos familiar from the logistic map [13]. For values of λ along the imaginary axis, we find that the map is stable if $\Im \lambda \in (-1/2, 1/2)$ and loses stability in a fold bifurcation at the exceptional points $\lambda = \pm i/2$. The full domain of convergence of the system is strictly larger than the RS disk, as shown in Figure 1. We also observe that the disk where both schemes converge, the dynamical scheme does so with a better rate than RS perturbation theory: we check that $|f^k(0) - x^*| \sim |1 - \sqrt{1 + 4\lambda^2}|^k = \mathcal{O}(|2\lambda^2|^k)$, while the remainder of the RS decays as $\mathcal{O}(|2\lambda|^k)$. This is a third way in which the dynamical scheme outperforms the usual RS series, at least in this case: not only is each iteration computationally cheaper, but the number of iterations required to reach a given precision is lower.

The set where IPT loses stability (the blue curve in Figure 1) can be computed as $4\lambda^2 + e^{it}(2 - e^{it}) = 0$ (same equation for both eigenvectors). The cusps of this curve are at $\lambda = \pm i/2$. In this particular case, the convergence circle of the RS perturbation theory is completely contained in the convergence domain of the iterative perturbation theory, and their boundaries intersect only at the cusp points. This convergence domain for IPT is directly related to the main cardioid of the classical Mandelbrot set: the set of complex values of the parameter c that lead to a bound trajectory of the classical quadratic (holomorphic) dynamical system $x^{(k+1)} = (x^{(k)})^2 + c$. The main cardioid of the Mandelbrot set (the domain of stability of a steady state) is bounded by the curve $4c - e^{it}(2 - e^{it}) = 0$. The boundary of the stability domain of our 2×2 example is simply a conformal transform of this cardioid by two complementary branches of the square root function composed with the sign inversion. The origin of this relation becomes obvious after the parameter change $c \mapsto -\lambda^2$ followed by the variable change $x \mapsto \lambda x$. This brings the classical system to the dynamical system of the only nontrivial component of the first line for our 2×2 example: $x^{(k+1)} = \lambda((x^{(k)})^2 - 1)$. The nontrivial component of the second line follows an equivalent (up to the sign change of the variable) equation: $x^{(k+1)} = \lambda(1 - (x^{(k)})^2)$.

3.4. Cusps and exceptional points. The link between the convergence of IPT and the singularities of the spectrum of M (as a function of the complex perturbation parameter λ) generalizes to higher dimensions. Consider a map F_n for some fixed n . An attracting equilibrium point of the corresponding dynamical system $z^{(k)} = F_n(z^{(k-1)})$ loses its stability when the Jacobian matrix $(\partial F_n)_{mk} \equiv \partial F_{mn} / \partial z_k$ of F_n has an eigenvalue (or *multiplier*) with absolute value equal to 1 at this point. The convergence domain of the dynamical system (2.3) for the whole matrix A of the eigenvectors is equal to the intersection of the convergence domains for its individual lines (2.2).

Consider the system of $N + 1$ polynomial equations of $N + 2$ complex variables (z_m for $1 \leq m \leq N$, λ , and μ)

$$\begin{cases} z = F_n(z), \\ \det(\partial F_n - \mu I) = 0. \end{cases}$$

The variable μ here plays the role of a multiplier of a steady state. Either by successively computing resultants or by constructing a Groebner basis with the correct lexicographical order, one can exclude the variables z_m from this system, which results in a single polynomial of two variables $(\lambda, \mu) \mapsto P(\lambda, \mu)$. This polynomial defines a complex 1-dimensional variety. The projection to the λ -plane of the real 1-dimensional variety defined by $\{P = 0, |\mu|^2 = 1\}$ corresponds to some curve C . A more informa-

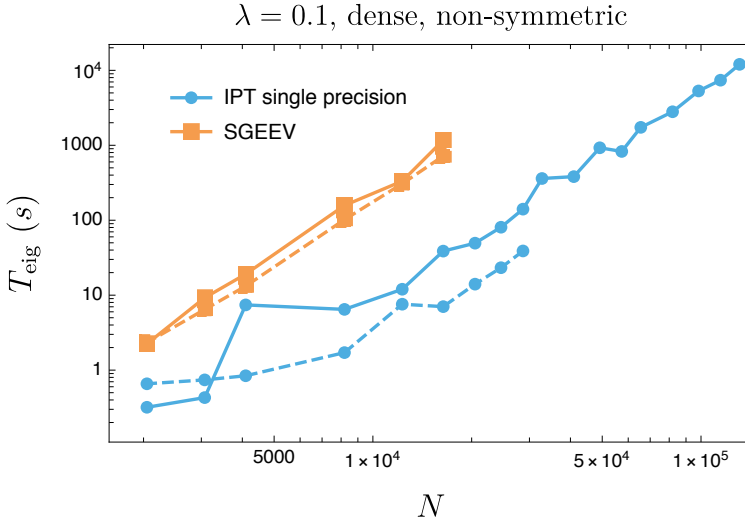


FIG. 2. Runtime vs. dimension N for dense, non-symmetric perturbative matrices of the form (4.1) in single precision. Blue lines refer to IPT and orange lines to LAPACK's GEEV routine, implemented on 128 CPU cores (continuous lines) or on a Titan V GPU (dashed lines). Within its perturbative convergence domain, IPT is up to 32 and 91 times faster than GEEV, respectively.

tive way is to represent this curve as a complex function of a real variable t implicitly defined by $P(\lambda, e^{it}) = 0$.

The curve C is the locus where a fixed point of F_n have a multiplier on the unit circle. In particular, the fixed point that at $\lambda = 0$ corresponds to $z_n = 1$ and $z_m = 0$, $m \neq n$, loses its stability along a particular subset of this curve. The convergence domain of the iterative perturbation theory is the domain that is bounded by these parts of the curve and that contains 0. It is possible to show that C is a smooth curve with cusps (return points), which correspond to the values of λ such that M has a nontrivial Jordan normal form (is non-diagonalizable), see Appendix F. In a typical case, all cusps are related to the merging of a pair of eigenvectors of M . For the dynamical system (2.2), the cusps, thus, correspond to the fold bifurcations of its steady states [14]. One of the multipliers equals to 1 at such merged point [15], so these values of λ can be found as a subset of the roots of the univariate polynomial $P(\lambda, 1)$. Not all its roots generally correspond to cusps and fold bifurcations, though, as demonstrated in E. On the other hand, all the cusps/fold bifurcation points are among the λ -roots of the discriminant polynomial $\text{Disc}_x \det(M - xI)$. These roots may correspond to both an actually defective matrix M (when two eigenvectors merge and M acquires a nontrivial Jordan normal form) and a simple degeneration of its eigenvalues (when two eigenvalues become equal but M retains a trivial Jordan normal form). Simple degenerations of eigenvalues are not related to cusps. Thus, the cusp points of C can be found as the intersection of the root sets of the two polynomials.

4. Performance. We now compare the efficiency and accuracy of IPT to reference eigenvalues routines. Our system consists of a dual AMD EPYC 7702 with 128 CPU cores using MATLAB (wrapping LAPACK and ARPACK) and a NVidia Titan

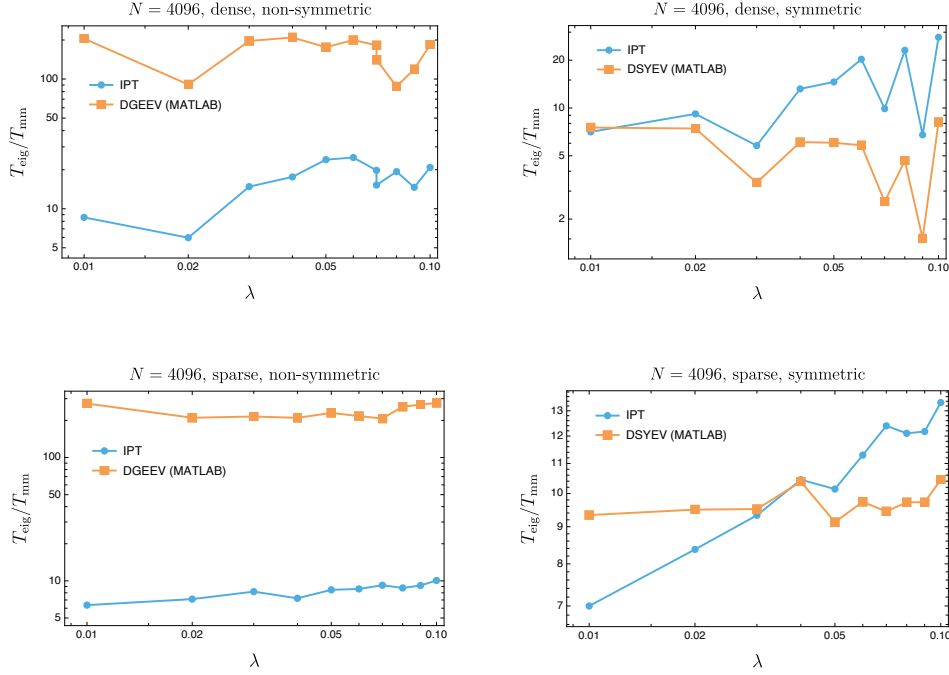


FIG. 3. *IPT* vs. *LAPACK* for the complete diagonalization of perturbative matrices with increasing λ , in double precision. The largest speed-ups are obtained for the non-symmetric problem.

V GPU using MAGMA [16] and Nvidia cuSOLVER. Test matrices are of the form

$$(4.1) \quad M = \text{diag}(n)_{1 \leq n \leq N} + \lambda R$$

where R is an array of standard normal random variables and λ a positive parameter. We consider four cases: R can either be dense or sparse (with density $50/N$, corresponding to $\sim 50N$ non-zero elements), and non-symmetric or symmetric (via $(R + R^T)/2$). For each case the time required to compute all N eigenpairs in double precision is denoted T_{eig} , and the time to compute the lowest-lying eigenpair is denoted T_{eigs} . As a reference we use the time for one matrix-matrix multiplication T_{mm} or one matrix-vector multiplication T_{mv} , respectively. In all figures below we use continuous lines for experiments on the CPU and dashed lines for experiments on the GPU, and brackets indicate the wrapper we used to call the relevant LAPACK or ARPACK routine.

4.1. Full spectrum. For the complete diagonalization problem we compare IPT to MATLAB's `eig` function, which calls LAPACK's routines GEEV for non-symmetric matrices and SYEV for symmetric matrices; on the GPU MAGMA is used instead.

Figure 3 shows the corresponding CPU timings in the dense, sparse, symmetric and non-symmetric cases ($N = 4096$). We make two observations. First, unlike LAPACK, our algorithm has a similar complexity with symmetric and non-symmetric matrices, leading to larger speed-ups in the latter case. Second, because it is based on matrix-matrix multiplication, IPT performs especially well on sparse matrices. This is another difference with standard full spectrum algorithms, which do not take

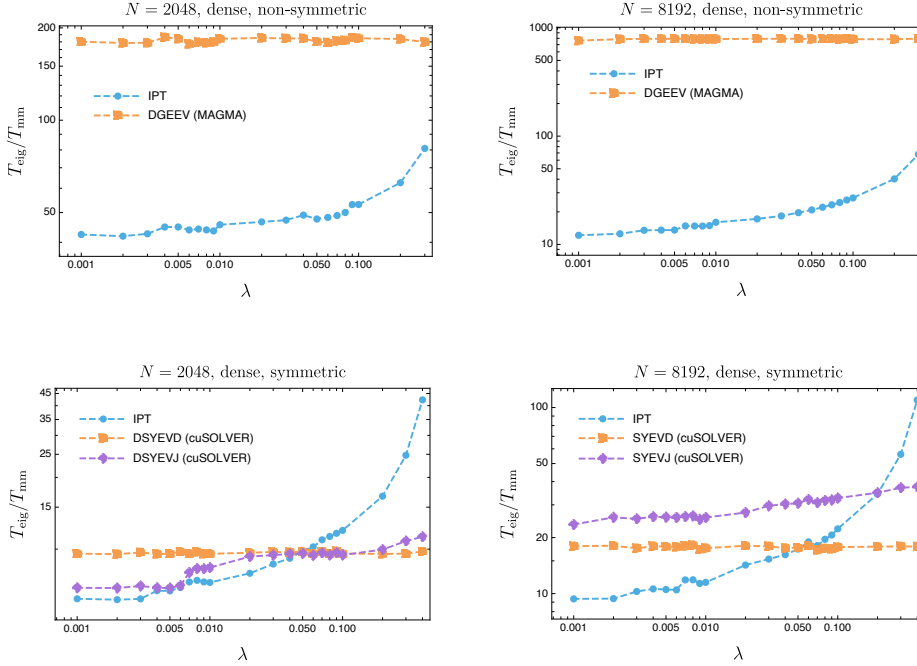


FIG. 4. Timing of full spectrum routines on the GPU for dense perturbative matrices. Here IPT proves to be faster than both Divide and Conquer (SYEVD) and Jacobi (SYEVJ) when λ is sufficiently small.

advantage of sparsity.

As noted earlier, Hessenberg reduction is inefficient for matrices which are already near diagonal. In the next experiment we compare IPT with Nvidia's GPU implementation of Jacobi's algorithm, which does not rely on reduction and is known to have local quadratic convergence. In spite of this advantage, Jacobi (labeled SYEVJ in cuSOLVER) only proved faster than divide-and-conquer SYEVD for small matrices sizes; for $N = 8182$ SYEVJ is slower than SYEVD for all values of λ (Figure 4, center and right panels). By contrast, our implementation of IPT in CUDA is faster than SYEVD for $\lambda \leq 0.05$. For dense, non-symmetric matrices, IPT is much faster than GEEV for all λ compatible with convergence (Figure 4, left panel).

4.2. One eigenpair. Next we consider the computation of just the lowest eigenpair of the matrices above, corresponding to the column $n = 1$. The reference routines here are the implicitly restarted Lanczos/Arnoldi methods in ARPACK [17] (**eigs** in MATLAB), and also the Davidson algorithm [5] for symmetric matrices (using the code from [18]).

Figure 5 presents our results. In all cases (dense, sparse, symmetric or non-symmetric) IPT runs much faster than ARPACK. Davidson, an algorithm designed for diagonally dominant matrices and used e.g. in quantum chemistry applications, provides a more meaningful reference point. Here we find that IPT is up to $\sim 5\times$ faster at small λ . This can be explained by the fact that, although IPT requires a similar number of iterations as Davidson, each iteration is cheaper, with just one

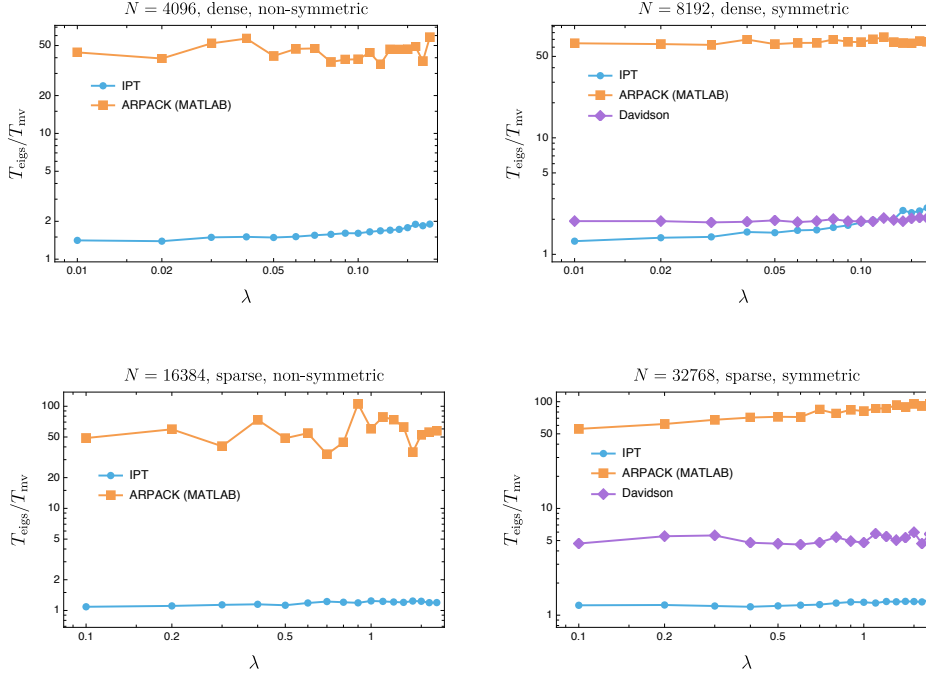


FIG. 5. *IPT vs. ARPACK (Lanczos/Arnoldi) and Davidson for the lowest-lying eigenpair of perturbative matrices of the form (4.1) and increasingly λ . Although Davidson is known to be especially fast for near-diagonal matrices, IPT is yet faster within its convergence domain.*

matrix-vector multiplication per step.

4.3. Parallelism. Underlying the performance of IPT is the high parallelism of matrix-vector and, especially, matrix-vector multiplication. Such parallelism is not shared by Householder reflections, which is why eigenvalue routines based on Hessenberg or tri-diagonal reduction do not scale as well on multi-core or GPU architectures. We illustrate this in Figure 6, where the time to diagonalize a dense, non-symmetric matrix with $\lambda = 0.1$ is plotted as a function of the number of active CPU cores. As expected from its simple structure, IPT parallelizes just as well as matrix-matrix multiplication (almost linearly in the number of cores). On large clusters with thousands of cores, we expect IPT will outperform GEEV by several orders of magnitude.

4.4. Accuracy. Finally we compared the accuracy of IPT on the full spectrum problem with LAPACK via MATLAB's `eig`. For this we used near-diagonal matrices of the form (4.1) with $N = 1024$ in double precision varying $\lambda \in [10^{-4}, 0.2]$. For each λ we ran IPT and `eig` to obtain the matrix of eigenvectors A and corresponding eigenvalues $E = \text{diag}(\varepsilon_n)_{1 \leq n \leq N}$. We then measured the accuracy of each routine through the residual error $\|MA - AE\|_F$, where $\|\cdot\|_F$ denotes the Frobenius norm. We find that IPT is more than an order of magnitude more accurate than LAPACK, with a median residual error of $4.4 \cdot 10^{-11}$ and $6.4 \cdot 10^{-10}$ respectively.

5. A mixed-precision eigenvalue algorithm. The condition that a matrix be near-diagonal of course severely restricts the applicability of IPT, although relevant

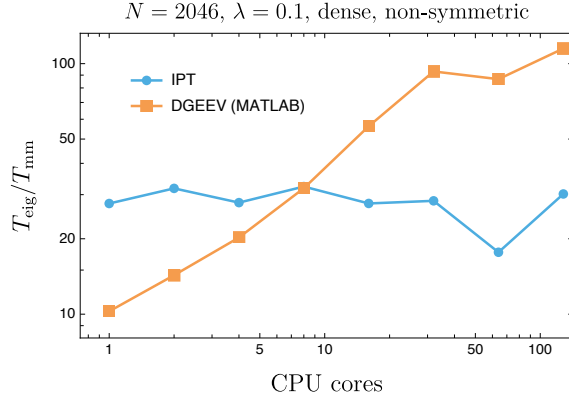


FIG. 6. *Parallel scaling.* Unlike direct methods based on Hessenberg reduction (here GEEV for a near-diagonal matrix of the form (4.1) with parameters as indicated), IPT scales as well as BLAS (here matrix-matrix multiplication). As a result, the speed-up of IPT over GEEV is only limited by the number of CPU cores available.

examples exist in quantum chemistry and elsewhere, as already mentioned. However, IPT can be used more generally as a *refinement* method for well-conditioned eigenvalue problems. Consider a generic matrix M with well separated eigenvalues, and assume given an approximation of its eigenmatrix A_0 . For instance, we could compute A_0 using standard drivers in single precision, resulting in a single precision eigenmatrix $A_{0,s}$. Next, we convert this matrix to double precision, denoted $A_{0,d}$, and apply IPT to the near-diagonal matrix $M' = A_{0,d}^{-1} M A_{0,d}$. Once iterations have converged to a new eigenmatrix A' , we can rotate back and obtain accurate eigenvectors for M as $A = A_{0,d} A'$. In practice the linear solve and matrix multiplication steps are fast, and so computing A takes about the same time as the low-precision diagonalization $A_{0,s}$.

Obviously, this method cannot be used for ill-conditioned eigenvalue problems, because then (i) θ becomes large and IPT ceases to converge, and (ii) the condition number of $A_{0,d}$ becomes large and accuracy is lost in the linear solve step. To measure the robustness of the mixed-precision algorithm to eigenvalue clustering, we considered matrices of the form

$$(5.1) \quad J_\alpha = Q^T D_\alpha Q \quad \text{with } D_\alpha = \text{diag}(10^{-\alpha n/N})_{1 \leq n \leq N},$$

where α is a parameter controlling the spacing between eigenvalues and Q a random orthogonal matrix. For matrices of size $N = 1024$ we found that IPT remained applicable up to $\alpha \simeq 4$, corresponding to a minimal spectral gap of $1.5 \cdot 10^{-6}$. (For this matrix **eigs** failed to converge with the default parameters.) For all values of α below this threshold, we obtain acceptable residual errors ($\sim 5x$ larger than DGEEV) and significant speed-ups over DGEEV (2 – 3x faster), see Figure 7.

6. Discussion. We have presented a new eigenvalue algorithm for near-diagonal matrices, be them symmetric or non-symmetric, dense or sparse. Its theoretical complexity is lower than that of standard methods (being equal to that of matrix-matrix multiplication for the full spectrum problem), as is its runtime for matrices of the form $\text{diag}(n)_n$ plus perturbation. Its structure is elementary: relying on machine-optimized BLAS routines for linear-algebraic operations, our program consists of less

Algorithm 5.1 Iterative refinement of eigenvectors of matrix M with well-separated eigenvalues

- 1: Compute eigenvectors $A_{0,s}$ in single precision *e.g.* using SGEEV or SSYEV
 - 2: Set $A_{0,d}$ as $A_{0,s}$ in double precision
 - 3: Compute $M' \leftarrow A_{0,d}^{-1} M A_{0,d}$ using a linear solver in double precision
 - 4: Compute eigenvectors A' and E using $\text{IPT}(M')$
 - 5: Return eigenvectors $A = A_{0,d} A'$
 - 6: Return eigenvalues E
-

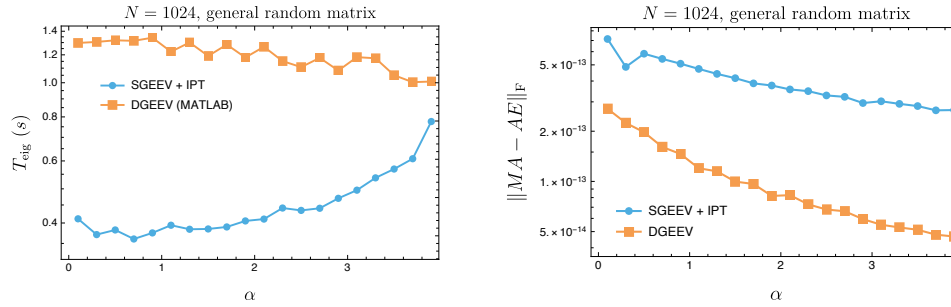


FIG. 7. *IPT* as a refinement algorithm for ill-conditioned problems (5.1) with increasingly small eigengap. Combining single-precision GEEV with *IPT* gives eigenvectors with acceptable accuracy at a fraction of the computational cost of double-precision GEEV.

than ten lines of python or MATLAB code. The largest speed-ups are obtained for non-symmetric problems.

We emphasize that the near-diagonality condition is quite restrictive: off-diagonal matrix elements must be small compared to diagonal spacings. In this regime Gershgorin's theorem already provides approximate information about the location of eigenvalues; it is fair to say, then, that *IPT* is more akin to a refinement procedure than a full-fledged eigenvalue algorithm. Even so *IPT* can be useful: using a mixed-precision approach we computed the eigenvectors of a general dense matrix with random entries to double precision in a fraction of the time required by DGEEV.

Future work should focus on stabilizing our procedure for larger perturbations. For instance, when the perturbation is too large and *IPT* blows up, we may shrink λ it to λ/Q for some integer Q , diagonalize the matrix with this smaller perturbation, restart the algorithm using the diagonal matrix thus obtained as initial condition, and repeat the operation Q times. This approach is similar to the homotopy continuation method for finding polynomial roots [19] and can effectively extend the domain of convergence of the present iterative scheme. Another idea is to leverage the projective-geometric structure outlined above, for instance by using charts on the complex projective space other than $z^n = 1$, which would lead to different maps with different convergence properties. A third possibility is to use the freedom in choosing the diagonal matrix D to construct maps with larger convergence domains, a trick which is known to sometimes improve the convergence of the RS series [11]. A fourth direction is to apply acceleration methods to speed up the convergence of fixed-point iteration. Preliminary tests using Anderson acceleration [20] suggest that significant speedups can be obtained in this way, at least for the one-eigenpair problem.

Acknowledgments. We thank Rostislav Matveev and Alexander Heaton for useful discussions.

REFERENCES

- [1] A. Szabo and N. S. Ostlund, *Modern Quantum Chemistry: Introduction to Advanced Electronic Structure Theory*. Dover Publications, 1996.
- [2] D. Pozar, *Microwave Engineering (2nd edition)*. Wiley, New York, 1998.
- [3] J. W. S. Rayleigh, *Theory of Sound. I (2nd ed.)*. London McMillan, 1894.
- [4] G. W. Stewart and J.-G. Sun, *Matrix Perturbation Theory*. Academic Press, New York, 1990.
- [5] E. R. Davidson, “The iterative calculation of a few of the lowest eigenvalues and corresponding eigenvectors of large real-symmetric matrices,” *Journal of Computational Physics*, vol. 17, pp. 87–94, jan 1975.
- [6] C. Lanczos, “An iteration method for the solution of the eigenvalue problem of linear differential and integral operators,” *Journal of Research of the National Bureau of Standards*, vol. 45, p. 255, oct 1950.
- [7] J. W. Demmel, *Applied Numerical Linear Algebra*. Society for Industrial and Applied Mathematics, 1997.
- [8] E. M. Lifshitz and L. D. Landau, *Quantum Mechanics: Non-relativistic Theory*. Pergamon Press, 1965.
- [9] M. Kenmoe, M. Smerlak, and A. Zadorin, “Iterative perturbation theory: physical and chemical applications,” *in preparation*, 2021.
- [10] T. Kato, *Perturbation Theory for Linear Operators*. Springer, 1995.
- [11] P. R. Surján and Á. Szabados, “Appendix to “Studies in Perturbation Theory”: The Problem of Partitioning,” in *Fundamental World of Quantum Chemistry*, pp. 129–185, Springer Netherlands, 2004.
- [12] R. A. Horn and C. R. Johnson, *Matrix Analysis*. Cambridge University Press, 2012.
- [13] R. M. May, “Simple mathematical models with very complicated dynamics,” *Nature*, vol. 261, pp. 459–467, jun 1976.
- [14] V. Dolotin and A. Morozov, “On the shapes of elementary domains, or why mandelbrot set is made from almost ideal circles?,” *International Journal of Modern Physics A*, vol. 23, pp. 3613–3684, sep 2008.
- [15] Y. A. Kuznetsov, *Elements of Applied Bifurcation Theory*. Springer, 2004.
- [16] S. Tomov, J. Dongarra, and M. Baboulin, “Towards dense linear algebra for hybrid GPU accelerated manycore systems,” *Parallel Computing*, vol. 36, pp. 232–240, jun 2010.
- [17] R. B. Lehoucq, D. C. Sorensen, and C. Yang, *ARPACK Users Guide: Solution of Large-Scale Eigenvalue Problems with Implicitly Restarted Arnoldi Methods*. Society for Industrial and Applied Mathematics, 1998.
- [18] Z. Jin, “davidson.” <https://www.mathworks.com/matlabcentral/fileexchange/71201-davidson>. Accessed on Fri, December 04, 2020.
- [19] A. Morgan, *Solving Polynomial Systems Using Continuation for Engineering and Scientific Problems*. Society for Industrial and Applied Mathematics, jan 2009.
- [20] H. F. Walker and P. Ni, “Anderson Acceleration for Fixed-Point Iterations,” *SIAM Journal on Numerical Analysis*, vol. 49, pp. 1715–1735, jan 2011.
- [21] P. Lax, “Linear algebra and its applications, john & sons,” *Inc., Hoboken, New Jersey*, 2007.
- [22] R. Roth and J. Langhammer, “Padé-resummed high-order perturbation theory for nuclear structure calculations,” *Physics Letters B*, vol. 683, pp. 272–277, jan 2010.

Appendix A. Eigenvectors and affine charts.

Let us start with the system of homogeneous polynomial equations

$$\mathcal{E}_{mn} : (Mz)_m z_n = (Mz)_n z_m$$

for all n and m . The projective variety defined by this full system is the union of the eigenvectors of M seen as projective points. In other words, the full system $\{\mathcal{E}_{mn}\}_{n,m}$ for all m and n (without assumptions $z_n \neq 0$) is equivalent to the initial eigenvector problem: it is the statement that the exterior product of Mz with z vanishes, which is equivalent to $\exists \varepsilon \, Mz = \varepsilon z$.

Assume that M belongs to a perturbative one-parameter family $M = D + \lambda \Delta$. Fix some n and consider the subset $\{\mathcal{E}_{mn}\}_m$ of equations that corresponds only to this n and to all $m \neq n$ ($N - 1$ equations in total). In the affine chart $U_n \simeq \mathbb{C}^{N-1}$ defined by $z_n = 1$, this subsystem becomes $z = F_n(z)$ with

$$(A.1) \quad F_n(z) = e_n + \theta_n \circ ((\Delta z)_n z - \Delta z).$$

The fixed points of this dynamical system are in one-to-one correspondence with the eigenvectors of M visible in this chart.

Indeed, we need to prove that for $z \in U_n$ the two following propositions are equivalent: (i) z is a root of $z = F_n(z)$ and (ii) $\exists \varepsilon \, Mz = \varepsilon z$. The (ii) \Rightarrow (i) direction is proven in the main text. The other direction is easy too. From $z_n = 1$ and $\{\mathcal{E}_{mn}\}_{n,m}$, we conclude that $(Mz)_m = (Mz)_n z_m$ for all $m \neq n$. If we now denote the common factor in these expressions as $\varepsilon = (Mz)_n$, then (ii) immediately follows.

It should be noted, however, that the correspondence holds only in the chart U_n . The system $\{\mathcal{E}_{mn}\}_m$ (for the fixed n , as before) may have other solutions in $\mathbb{C}P^{N-1}$, but all of them by necessity are at infinity in U_n . These solutions are not related to the eigenvectors of M . Indeed, consider $\{\mathcal{E}_{mn}\}_m$ in the form

$$(A.2) \quad z_n z_m = \lambda \theta_{mn} (z_m (\Delta z)_n - z_n (\Delta z)_m),$$

for some fixed n and set $z_n = 0$ to find solutions in $\mathbb{C}P^{N-1}$ that are at infinity in U_n . Clearly, any z with $z_n = 0$ that obeys $(\Delta z)_n = 0$ is a solution of (A.2). Thus, in general, there is a whole $(N - 3)$ -dimensional complex projective subspace of such solutions in $\mathbb{C}P^{N-1}$ (corresponding to a $(N - 2)$ -dimensional complex hyperplane in the affine space \mathbb{C}^N).

Finally, at $\lambda = 0$ there is only one solution in each chart U_n for each corresponding system $\{\mathcal{E}_{mn}\}_m$, namely the origin of the chart (which represents the corresponding unperturbed eigenvector), while for generic value of λ , D and Δ there are all N solutions in each chart for its corresponding system of equations. As soon as λ becomes different from 0, the other $N - 1$ solutions appear in the chart from infinity.

Appendix B. Fixed points have full rank.

As in the main text, we consider a square $N \times N$ matrix M and its splitting $M = D + \Delta$, where $D = \mathcal{D}(M)$ is its diagonal part and Δ is its off-diagonal part. The set of solutions of equation $A = F(A)$, where F is defined by matrix M , contains matrices composed of all combinations of eigenvectors of M with the appropriate normalization (the n -th coordinate of the column at the n -th position is set to 1). Naturally, some solutions are more informative than others, as some solutions may contain several repeated eigenvectors. Such solutions are singled out by their dropped rank, viz. $\text{rank}(A) < N$. In principle, there is a danger that the iterative algorithms

converges to one such solutions with a loss of information about the eigenvectors of M as a result. We show in this section that this never happens under the sufficient condition of convergence presented in the main text.

We remind that F is defined via Δ and θ , the matrix of inverse diagonal entry gaps of M . In the main text we prove that any matrix M that obeys condition

$$(B.1) \quad \|\theta\| \cdot \|\Delta\| < 3 - 2\sqrt{2}$$

has a unique solution A^* of $A = F(A)$ in the ball $B_{\sqrt{2}}(I)$ (the norm is spectral) and this solution is a stable fixed point of iterations of F . We now show that this unique solution always contains the full information on eigenvectors of M , i.e. the columns of A^* form an eigenbasis of M .

THEOREM B.1. *Let matrix M obey condition (B.1) and A^* be the unique fixed point of F in $B_{\sqrt{2}}(I)$. Then A^* has full rank.*

We will need one additional theorem and two lemmas.

THEOREM B.2 ([21] Theorem 8, page 130). *Let M_λ be a differentiable matrix-valued function of real λ , a_λ an eigenvalue of M_λ of multiplicity one. Then we can choose an eigenvector h_λ of M_λ pertaining to the eigenvalue a_λ to depend differentiably on λ .*

The theorem guarantees that the eigenvector corresponding to an eigenvalue with multiplicity one is at least a continuous function of the parameter as a projective space valued function.

LEMMA B.3. *Let M be a matrix that obeys (B.1). Then there are no eigenvectors of M from eigenspaces of dimension higher than one as columns of the corresponding unique A^* in $B_{\sqrt{2}}(I)$.*

Proof. If A^* contains an eigenvector from an eigenspace of M with dimension higher than one, then any matrix A obtained by a substitution in A^* of that eigenvector with a vector from this eigenspace is a fixed point of F , too. This means that there is a whole subspace of fixed points of F of dimension higher than zero which includes A^* . But this contradicts the uniqueness of A^* in $B_{\sqrt{2}}(I)$. \square

LEMMA B.4. *If M obeys (B.1) and is defective, then A^* does not contain any eigenvector causing the defect.*

Proof. By Lemma (B.3), it is enough to assume that M does not have geometrically multiple eigenvalues and all its eigenvectors are isolated projective points, so all fixed points of F are isolated matrices. Let such M be defective. Let J be a Jordan normal form of M and S be the transition matrix that turns M into J . Consider a deformation J_μ of J given by $J_\mu = J + \text{diag}(\mu)$, where $\mu \in \mathbb{C}^N$. This induces a deformation of M given by $M_\mu = M + S \text{diag}(\mu) S^{-1}$. It is clear that one can find arbitrarily small μ such that all diagonal entries of J_μ are different. As J_μ is upper triangular, its eigenvalues, and thus those of M_μ , are equal to its diagonal entries. But then M_μ has a full eigenbasis of isolated eigenvectors. The formerly merged eigenvectors split into distinct ones. Furthermore, the new eigenvectors that split from an old defective eigenvector can be made arbitrarily close to it (as projective points) by choosing μ small enough. This is obvious from considering the eigenvectors of J_μ and their behavior at the limit $\mu \rightarrow 0$. The nondefective eigenvectors, in turn, do not change.

All this implies that there is a deformation M_μ of M such that $\|M_\mu - M\|$ is arbitrarily small and thus (B.1) still holds for θ and Δ computed for M_μ . At the

same time, A^* splits into several arbitrarily close, and thus still contained in $B_{\sqrt{2}}(I)$ for small enough μ , fixed points of F , with two or more of them being full-rank and multiple associated lower rank fixed points. But this contradicts the uniqueness of the fixed point of F computed for the deformed matrix M_μ . \square

Proof of Theorem (B.1). A square matrix is rank-deficient if either two of its columns are collinear or more than two of its columns are linearly dependent but not pairwise collinear. For A^* the latter is only possible if the corresponding eigenvectors belong to an eigenspace of M of dimension higher than one, which is ruled out by Lemma (B.3). By Lemma (B.4), A^* does not contain any defective eigenvectors of M . Then the rank can be lost only by a repeat of an eigenvector (with renormalization) corresponding to an eigenvalue of multiplicity one.

Embed M into the perturbative family $M_\lambda = D + \lambda\Delta$ with $\lambda \in [0, 1]$, so that $M_1 = M$ and $M_0 = D$. It follows that M_λ obeys $\|\theta_\lambda\| \cdot \|\Delta_\lambda\| < 3 - 2\sqrt{2}$ for all λ , where $\theta_\lambda = \theta$ the matrix of inverse gaps of $D_\lambda = \mathcal{D}(M_\lambda) = D$ and $\Delta_\lambda = M_\lambda - D_\lambda = \lambda\Delta$. Thus, each M_λ has a unique fixed point A_λ^* of the corresponding F_λ in $B_{\sqrt{2}}(I)$. Furthermore, by Lemmas (B.3) and (B.4) we can be sure that none of the columns of A_λ^* for each value of λ corresponds either to an eigenvector with algebraic multiplicity higher than one or lays in an eigenspace of M_λ with dimension higher than one. Thus they all correspond to eigenvalues that are simple roots of the characteristic polynomial of M_λ . Then all projective points that induce columns of A_λ^* are differentiable functions of λ by Theorem (B.2). It means that if some two columns of $A^* = A_\lambda^*$ are collinear (and thus correspond to the same projective point), the same columns stay collinear in A_λ^* for all λ . But none of the columns of $A_\lambda^* = I$ are collinear. We conclude that A^* cannot have collinear columns. \square

COROLLARY B.5. *If M has eigenvalues with multiplicity higher than one, then $\|\theta\| \cdot \|\Delta\| \geq 3 - 2\sqrt{2}$ in any basis, where θ is defined.*

Appendix C. Rayleigh-Schrödinger perturbation theory.

Here we recall the derivation of the Rayleigh-Schrödinger recursion, given *e.g.* in [22]. Let ε_n and $z_{(n)}$ respectively be the n -th eigenvalue and eigenvector of $M = D + \lambda\Delta$ corresponding to the unperturbed eigenvalues ϵ_n and eigenvector e_n , chosen so that $\lim_{\lambda \rightarrow 0} z_{(n)} = e_n$ and $\langle e_n, z_{(n)} \rangle = 1$ for all λ (a choice known as “intermediate normalization”). We start by expanding these in powers of λ :

$$\varepsilon_n = \sum_{\ell \geq 0} \lambda^\ell \varepsilon_n^{(\ell)} \quad \text{and} \quad z_{(n)} = \sum_{\ell \geq 0} \lambda^\ell z_{(n)}^{(\ell)}.$$

Substituting these ansätze into the eigenvalue equation $Mz = \varepsilon z$ and making use of the Cauchy product formula, this yields $Dz_{(n)}^{(0)} = \varepsilon_n^{(0)} z_{(n)}^{(0)}$ at zeroth order (hence $\varepsilon_n^{(0)} = \epsilon_n$) and for $\ell \geq 1$

$$(D - \epsilon_n)z_{(n)}^{(\ell)} = \sum_{s=1}^{\ell} \varepsilon_n^{(s)} z_{(n)}^{(\ell-s)} - \Delta z_{(n)}^{(\ell-1)}.$$

It is convenient to expand $z_{(n)}^{(\ell)}$ in the basis of the eigenstates of D as $z_{(n)}^{(\ell)} = \sum_{m=1}^N a_{mn}^{(\ell)} e_m$ with $a_{nn}^{(0)} = \delta_{nn}$ and $a_{nn}^{(\ell)} = 0$ for $\ell \geq 1$. This gives for each $\ell \geq 1$ and $1 \leq m \leq N$

$$(\epsilon_m - \epsilon_n)a_{mn}^{(\ell)} = \sum_{s=1}^{\ell} \varepsilon_n^{(s)} a_{mn}^{(\ell-s)} - (\Delta a^{(\ell-1)})_{mn}.$$

The equation for the eigenvalues correction is extracted by setting $m = n$ in this equation and using $a_{nn}^{(\ell)} = \delta_{\ell,0}$. This leads to $\varepsilon_n^{(\ell)} = (\Delta a^{(\ell-1)})_{nn}$. Injecting this back into the equation above we arrive at

$$(C.1) \quad a_{mn}^{(\ell)} = \theta_{mn} \left(\sum_{s=1}^{\ell} (\Delta a^{(s-1)})_{nn} a_{mn}^{(\ell-s)} - (\Delta a^{(\ell-1)})_{mn} \right).$$

Appendix D. Iterative perturbation theory contains the RS series.

We prove $A^{(k)} = A_{\text{RS}}^{(k)} + \mathcal{O}(\lambda^{k+1})$ by induction. Obviously $A^{(0)} = A_{\text{RS}}^{(0)} = I$. Suppose that $A^{(k-1)} = A_{\text{RS}}^{(k-1)} + \mathcal{O}(\lambda^k)$ or, more specifically,

$$A^{(k-1)} = \sum_{\ell=0}^{k-1} \lambda^{\ell} a^{(\ell)} + \mathcal{O}(\lambda^k),$$

where the matrices $a^{(\ell)}$ satisfy the recursion C.1. Then from $A^{(k)} = F(A^{(k-1)})$ we have

$$A^{(k)} = I + \lambda \theta \circ \left(\sum_{m=0}^{k-1} \lambda^m a^{(m)} \mathcal{D} \left(\sum_{\ell=0}^{k-1} \lambda^{\ell} \Delta a^{(\ell)} \right) - \sum_{\ell=0}^{k-1} \lambda^{\ell} \Delta a^{(\ell)} \right) + \mathcal{O}(\lambda^{k+1}).$$

From this expression it is easy to see that the term of s -th order in λ in $A^{(k)}$ is given by terms with $\ell + m = s - 1$, viz.

$$\lambda^s \theta \circ \left(\left(\sum_{\ell=0}^{s-1} a^{(s-1-\ell)} \mathcal{D} \left(\Delta a^{(\ell)} \right) \right) - \Delta a^{(s-1)} \right).$$

This term matches exactly the RS correction term $\lambda^s a^{(s)}$. This concludes the proof.

Appendix E. Further explicit examples.

The 2×2 example in the main text is very special. In fact, any 2-dimensional case is special in the following sense. The iterative approximating sequence for $M = D + \lambda \Delta$ for any D and Δ takes the form

$$A^{(k)} = \begin{pmatrix} 1 & f_1^k(0) \\ f_2^k(0) & 1 \end{pmatrix},$$

where f_j are univariate quadratic polynomial functions related by $g_1(x) = x^2 g_2(1/x)$, with $g_j(x) \equiv x - f_j(x)$. The first special feature of this recursion scheme is that it is equivalent to a 1-dimensional quadratic discrete-time dynamical system for each column of A . This implies that the only critical point of either f_j (0, when the diagonal elements of Δ are equal) is necessarily attracted by at most unique stable fixed point. The second special feature is fact that both columns have exactly the same convergence domains in the λ -plane. To see this, suppose that x_1 and x_2 are the roots of g_1 . Then it follows that $1/x_1$ and $1/x_2$ are the roots of g_2 . As $g_2'(1/x) = 2g_1(x)/x - g_1'(x)$, and (like for any quadratic polynomial) $g_1'(x_1) = -g_1'(x_2)$, we also see that $g_1'(x_{1,2}) = g_2'(1/x_{2,1})$, and thus $f_1'(x_{1,2}) = f_2'(1/x_{2,1})$. Therefore, the fixed point of the dynamical systems defined by $x^{(k+1)} = f_1(x^{(k)})$ corresponding to an eigenvector and the fixed point of $x^{(k+1)} = f_2(x^{(k)})$ corresponding to the different eigenvector are stable or unstable simultaneously.

These two properties are not generic when $N > 2$. Therefore, we provide another explicit example of a 3×3 matrix to foster some intuition for more general cases:

$$M = \begin{pmatrix} 0 & 0 & 0 \\ 0 & 1 & 0 \\ 0 & 0 & 3 \end{pmatrix} + \lambda \begin{pmatrix} 0 & 1 & 2 \\ 1 & 0 & 3 \\ 2 & 3 & 0 \end{pmatrix}.$$

The polynomial P that defines the fixed point degeneration curve C here takes the form for $n = 1$

$$\begin{aligned} P(\lambda, \mu) = & 63792\lambda^7 - 28352\lambda^6\mu - 68040\lambda^6 - 29556\lambda^5\mu^2 + 89352\lambda^5\mu \\ & - 13239\lambda^5 + 960\lambda^4\mu^3 + 14516\lambda^4\mu^2 - 39164\lambda^4\mu + 12116\lambda^4 \\ & + 5616\lambda^3\mu^4 - 26658\lambda^3\mu^3 + 29988\lambda^3\mu^2 - 546\lambda^3\mu - 2448\lambda^3 \\ & + 468\lambda^2\mu^5 - 3720\lambda^2\mu^4 + 12820\lambda^2\mu^3 - 17648\lambda^2\mu^2 + 7584\lambda^2\mu \\ & - 1296\lambda^2 - 243\lambda\mu^6 + 1404\lambda\mu^5 - 2619\lambda\mu^4 + 1350\lambda\mu^3 + 432\lambda\mu^2 \\ (E.1) \quad & + 108\mu^6 - 792\mu^5 + 1980\mu^4 - 1872\mu^3 + 432\mu^2, \end{aligned}$$

for $n = 2$

$$\begin{aligned} P(\lambda, \mu) = & 113408\lambda^7 - 63792\lambda^6\mu - 120960\lambda^6 + 7416\lambda^5\mu^2 + 53208\lambda^5\mu \\ & + 36424\lambda^5 + 6525\lambda^4\mu^3 - 11034\lambda^4\mu^2 - 13824\lambda^4\mu - 5664\lambda^4 \\ & - 3156\lambda^3\mu^4 - 2472\lambda^3\mu^3 + 10332\lambda^3\mu^2 + 3696\lambda^3\mu + 3088\lambda^3 \\ & - 72\lambda^2\mu^5 + 1800\lambda^2\mu^4 - 1800\lambda^2\mu^3 - 2088\lambda^2\mu^2 - 1296\lambda^2\mu \\ & - 576\lambda^2 + 128\lambda\mu^6 - 24\lambda\mu^5 - 736\lambda\mu^4 - 120\lambda\mu^3 + 1328\lambda\mu^2 \\ (E.2) \quad & - 72\mu^6 + 108\mu^5 + 360\mu^4 - 432\mu^3 - 288\mu^2, \end{aligned}$$

and for $n = 3$

$$\begin{aligned} P(\lambda, \mu) = & 35440\lambda^7 - 42528\lambda^6\mu - 37800\lambda^6 - 32360\lambda^5\mu^2 + 110080\lambda^5\mu \\ & - 23295\lambda^5 + 29112\lambda^4\mu^3 - 4800\lambda^4\mu^2 - 88614\lambda^4\mu + 51024\lambda^4 \\ & + 14640\lambda^3\mu^4 - 78760\lambda^3\mu^3 + 116760\lambda^3\mu^2 - 52920\lambda^3\mu + 5400\lambda^3 \\ & - 2376\lambda^2\mu^5 - 10152\lambda^2\mu^4 + 70296\lambda^2\mu^3 - 101496\lambda^2\mu^2 + 41904\lambda^2\mu \\ & - 864\lambda^2 - 1080\lambda\mu^6 + 7920\lambda\mu^5 - 19620\lambda\mu^4 + 19440\lambda\mu^3 - 6480\lambda\mu^2 \\ (E.3) \quad & + 1296\mu^6 - 7992\mu^5 + 17712\mu^4 - 16416\mu^3 + 5184\mu^2. \end{aligned}$$

As we can see, the dynamical systems for all three columns of A ($n = 1, 2, 3$) have different domains of convergence in the λ plane. The corresponding curves are depicted on [Figure 8](#), [Figure 9](#), and [Figure 10](#), respectively.

There are differences also in curves for individuals columns with those for the 2×2 case. Note that a curve C does not contain enough information to find the convergence domain itself. The domains on [Figure 8–Figure 10](#) were found empirically. Of course, they are bound by some parts of C and include the point $\lambda = 0$. The reason for some parts of C not forming the boundary of the domain is that its different parts

correspond to different eigenvectors. In other words, they belong to different branches of a multivalued eigenvector function of λ , the cusps being the branching points.

Consider as a particular example the case $n = 2$. The curve C intersects itself at $\lambda \approx -0.49$. Above the real axis about this point, one of the two intersecting branches of the curve form the convergence boundary. Below the real axis, the other one takes its place. This indicates that the two branches correspond to different multipliers of the same fixed point. When $\Im \lambda > 0$, one of them crosses the unitary circle at the boundary of the convergence domain; when $\Im \lambda < 0$, the other one does. At $\lambda \approx -0.49$, both of them cross the unitary circle simultaneously. This situation corresponds, thus, to a Neimark-Sacker bifurcation (the discrete time analog of the Andronov-Hopf bifurcation). Both branches are in fact parts of the same continuous curve that passes through the point $\lambda \approx 0.56$. Around this point, the curve poses no problem to the convergence of the dynamical system. The reason for this is that an excursion around cusps (branching points of eigenvectors) permutes some eigenvectors. As a consequence, the curve at $\lambda \approx -0.49$ corresponds to the loss of stability of the eigenvector that is a continuation of the unique stable eigenvector at $\lambda = 0$ by the path $[0, -0.49]$. At the same time, the same curve at $\lambda \approx 0.56$ indicates a unitary by absolute value multiplier of an eigenvector that is not a continuation of the initial one by the path $[0, 0.56]$.

Not all features of the curves depicted this 3×3 case are generic either. The particular symmetry with respect to the complex conjugation of the curve and of its cusps is not generic for general complex matrices D and Δ , but it is a generic feature of matrices with real components. In this particular case, due to this symmetry, the only possible bifurcations for real values of λ are the flip bifurcations (a multiplier equals to -1 , typically followed by the cycle doubling cascade), the Neimark-Sacker bifurcation (two multipliers assume complex conjugate values $e^{\pm it}$ for some t), and, if the matrices are not symmetric, the fold bifurcation (a multiplier is equal to 1). With symmetric real matrices, the fold bifurcation is not encountered because the cusps cannot be real but instead form complex conjugated pairs. These features are the consequence of the behavior of $\det(D + \lambda\Delta - xI)$ with respect to complex conjugation and from the fact that symmetric real matrices cannot have nontrivial Jordan forms.

Likewise, Hermitian matrices result in complex conjugate nonreal cusp pairs, but the curve itself is not necessarily symmetric. As a result, there are many more ways for a steady state to lose its stability, from which the fold bifurcation is, however, excluded. Generic bifurcations at $\lambda \in \mathbb{R}$ here consist in a multiplier getting a value e^{it} for some $t \neq 0$. The situation for general complex matrices lacks any symmetry at all. Here steady states lose their stability by a multiplier crossing the unit circle with any value of t , and thus the fold bifurcation, although possible, is not generic. It is generic for one-parameter (in addition to λ) families of matrices.

As already noted, for the holomorphic dynamics of any 2×2 case the unique critical point is guaranteed to be attracted by the unique attracting periodic orbit, if the latter exists. This, in turn, guarantees that for any Δ with zero diagonal the iteration of F starting from the identity matrix converges to the needed solution provided that λ is in the convergence domain. This is not true anymore for $N > 2$, starting already from the fact that there are no discrete critical points in larger dimensions. The problem of finding a good initial condition becomes non-trivial. As can be seen on [Figure 9](#), the particular 3×3 case encounters this problem for the second column ($n = 2$). The naive iteration with $A^{(0)} = I$ does not converge to the existing attracting fixed point of the dynamical system near some boundaries of its convergence domain. Our current understanding of this phenomenon is the crossing

of the initial point by the attraction basin boundary (in the z -space). This boundary is generally fractal. Perhaps this explains the eroded appearance of the empirical convergence domain of the autonomous iteration.

To somewhat mitigate this complication, we applied a nonautonomous iteration scheme in the form, omitting details, $z^{(k+1)} = F_2(z^{(k)}, \lambda(1 - \alpha^k))$ with $z^{(0)} = (0, 1, 0)$, where α is some positive number $\alpha < 1$, so that $\lim_{k \rightarrow \infty} \lambda(1 - \alpha^k) = \lambda$, and we explicitly indicated the dependence of $F_2(z, \lambda)$ on λ . The idea of this *ad hoc* approach is the continuation of the steady state in the extended (z, λ) -phase space from values of λ that put $z^{(0)}$ inside the convergence domain of that steady state. Doing so, we managed to empirically recover the theoretical convergence domain (see [Figure 9](#)).

Finally, we would like to point out an interesting generic occurrence of a unitary multiplier without the fold bifurcation. For $n = 1$, this situation takes place at $\lambda \approx 0.45$, for $n = 2$ at $\lambda \approx 0.56$, and for $n = 3$ at $\lambda \approx 1.2$. All three points are on the real axis, as is expected from the symmetry considerations above. There is no cusp at these points and no fold bifurcations (no merging of eigenvectors), as it should be for symmetric real matrices. Instead, another multiplier of the same fixed point goes to infinity at the same value of λ (the point becomes super-repelling). As a result, the theorem of the reduction to the central manifold is not applicable.

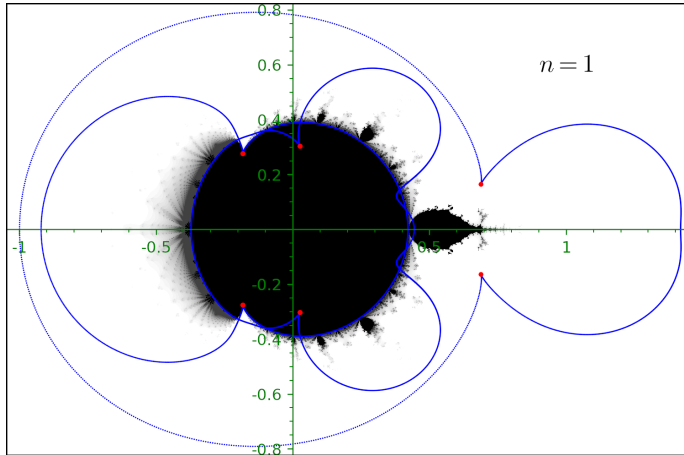


FIG. 8. The convergence domain on the λ -plane for the first column of A (the first eigenvector z_1) for the 3×3 example. The Mandelbrot-like set (domain where orbits remain bounded) of the iterative scheme is shown in black and grey. The empirical convergence domain is shown in black. Its largest component corresponds to the stability of a steady state (the applicability domain of the iterative method). Small components correspond to stability of various periodic orbits. Various shades of grey show the values of λ that lead to divergence to infinity (the darker the slower the divergence). In red are the values of λ where the matrix is non-diagonalizable.

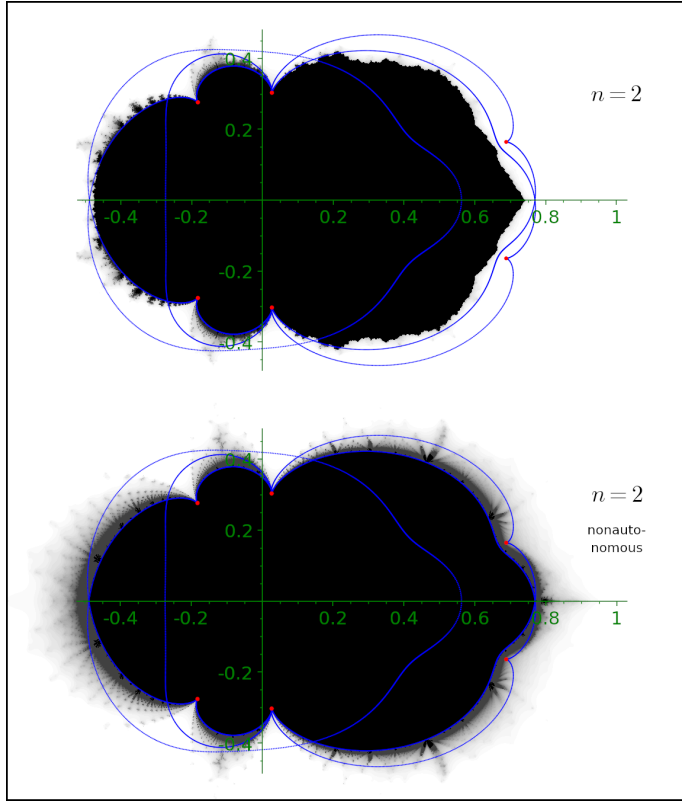


FIG. 9. Same as Figure 8 for the second eigenvector z_2 (the second column of A). Small components correspond to stability of various periodic orbits. Various shades of grey show the values of λ that lead to divergence to infinity (the darker the slower the divergence).

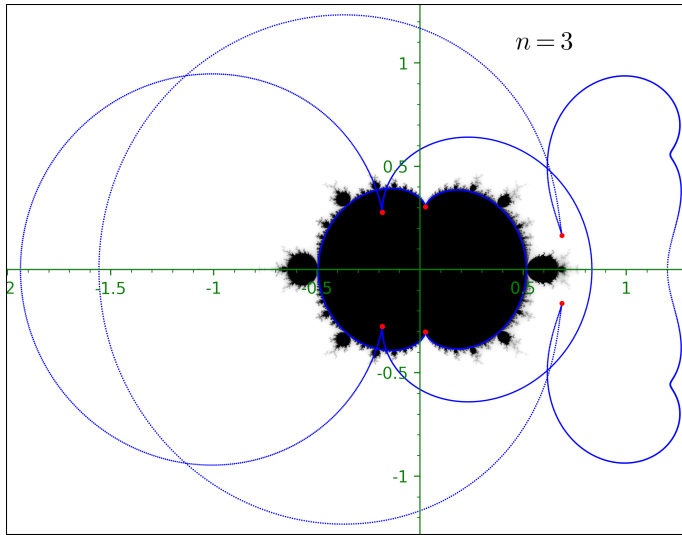


FIG. 10. Same as Figure 8 for the third eigenvector z_3 (the third column of A).

Appendix F. Exceptional points and cusps of C .

We will prove that if M is defective at some value of λ , then $d\lambda/dt = 0$ for the curve C at that point (as above, μ is a multiplier of the dynamical perturbation theory and C is defined by $\mu = e^{it}$ and is locally considered as a curve $t \mapsto \lambda(t)$).

Fix n and consider the dynamical system for the n -th column only. Let $x = (x_1, \dots, x_{N-1})$ be a tuple of affine coordinates in the affine chart U_n . Note that the coordinates are rearranged in comparison to z_j : $x_1 = z_1, \dots, x_{n-1} = z_{n-1}, x_n = z_{n+1}, \dots, x_{N-1} = z_N$. We consider the representation of the corresponding dynamical system in U_n too. Let it be given by the tuple of functions $f = (f_1, \dots, f_{N-1})$ that correspond to functions F_{jn} with F_{nn} omitted (F_{nn} is trivially 1 in U_n). The same rearrangement is implied for f_j as for x_j . Thus, the dynamical system is defined by $x^{(k+1)} = f(x^{(k)})$ and the stationary states are defined by the system of equations $x = f(x)$.

Consider \mathbb{C}^{N+1} with coordinates $(x_1, \dots, x_{N-1}, \lambda, \nu)$, where $\nu \equiv \mu - 1$, as a complex analytic manifold with these coordinates as global holomorphic coordinates on it. Let us define polynomial functions

$$\mathcal{F}_j: \mathbb{C}^{N+1} \rightarrow \mathbb{C}, (x, \lambda, \nu) \mapsto f_j(x, \lambda) - x_j,$$

and $\mathcal{F} = (\mathcal{F}_1, \dots, \mathcal{F}_{N-1})$. Let us denote $J \equiv \frac{\partial \mathcal{F}}{\partial x} \equiv \frac{\partial(\mathcal{F}_1, \dots, \mathcal{F}_{N-1})}{\partial(x_1, \dots, x_{N-1})}$ the Jacobian matrix of \mathcal{F} with respect to variables x_j . Let I be the unitary $(N-1) \times (N-1)$ matrix.

Consider the complex 1-dimensional variety $\mathcal{C} \subset \mathbb{C}^{N+1}$ defined by the polynomial system

$$\begin{cases} \mathcal{F} = 0, \\ \det(J - \nu I) = 0. \end{cases}$$

Curve C is the projection to the λ -plane of the real 1-dimensional variety $\tilde{C} = \mathcal{C} \cap \{|\nu + 1|^2 = 1\}$ in \mathbb{C}^{N+1} considered as $\mathbb{R}^{2(N+1)}$.

First, note that if M is defective at some value of λ , then the system of equations $\mathcal{F} = 0$ (with this values of λ fixed and considered for unknowns $x \in \mathbb{C}^{N-1}$) has a root x of multiplicity greater than 1. This means that the hyperplanes $\{\mathcal{F}_j = 0\}$ are not in general position at the intersection that corresponds to this root, which implies $\det \partial \mathcal{F} / \partial x = 0$. Therefore, the point $p \in \mathbb{C}^{N+1}$ with the same x and λ and with $\nu = 0$ belongs to \mathcal{C} and represents this non-diagonalizability of M .

Let d denote the exterior derivative on the complex of holomorphic exterior forms $\Omega^\bullet(\mathbb{C}^{N+1})$. Alternatively, one may treat it in purely axiomatic way as the Kähler differential on the algebra of holomorphic functions on \mathbb{C}^{N+1} with the appropriate factorization in the end. Let $p \in \mathcal{C}$ be a point of geometric degeneration of M with $\nu = 0$ as above.

THEOREM F.1. *Assume that the following nondegeneration condition holds: $d_p \det J \wedge \bigwedge_j d_p \mathcal{F}_j \neq 0$. Then \mathcal{C} can be locally parametrized by ν around p and, with this parametrization, $d\lambda/d\nu = 0$ at p .*

Proof. Let $T_p \mathbb{C}^{N+1}$ be the holomorphic tangent space to \mathbb{C}^{N+1} at p , that is the tangent space spanned by the holomorphic vector fields $\partial_j \equiv \partial/\partial x_j$, $\partial_\lambda \equiv \partial/\partial \lambda$, $\partial_\nu \equiv \partial/\partial \nu$ at p . Let us denote $\iota_u \sigma_p$ the contraction of a holomorphic form σ ($\sigma_p \in \bigwedge_p^\bullet \mathbb{C}^{N+1}$) with a tangent vector $u \in T_p \mathbb{C}^{N+1}$ at point p .

Let us denote $\omega_p \equiv d_p \det(J - \nu I) \wedge \bigwedge_j d_p \mathcal{F}_j$ and $\varpi_p \equiv d_p \det J \wedge \bigwedge_j d_p \mathcal{F}_j$. By the premise, $\varpi_p \neq 0$, which also implies $\omega_p \neq 0$. Indeed, the free term (with respect to ν) of the polynomial $\det(J - \nu I)$ is equal to $\det J$, and thus

$$(F.1) \quad d_p \det(J - \nu I) = \partial_\nu \det(J - \nu I)|_p d_p \nu + d_p \det J,$$

where the two terms are linearly independent because $\partial_\nu \det J = 0$. Therefore, as non of \mathcal{F}_j depends on ν , ω_p differs from ϖ_p by an addition of a linearly independent term.

Let $v \in T_p \mathbb{C}^{N+1}$ be a nonzero vector with coordinates (v^i, v^λ, v^ν) tangent to \mathcal{C} . It means that $v \det(J - \nu I) = v \mathcal{F}_j = 0$. This, in turn, implies $\iota_v \omega_p = 0$.

As all \mathcal{F}_j depend only on x and λ , we have $d_p \lambda \wedge \bigwedge_j d_p \mathcal{F}_j = \det J|_p d_p \lambda \wedge \bigwedge_j d_p x_j = 0$, and thus $d_p \lambda \wedge \omega_p = 0$. Therefore, we have

$$\iota_v(d_p \lambda \wedge \omega_p) = -d_p \lambda \wedge \iota_v \omega_p + v^\lambda \omega_p = v^\lambda \omega_p = 0.$$

This implies $v^\lambda = 0$.

On the other hand, by (F.1) we have

$$d_p \nu \wedge d_p \det(J - \nu I) = d_p \nu \wedge d_p \det J,$$

and thus $d_p \nu \wedge \omega_p = d_p \nu \wedge \varpi_p \neq 0$. But $d\nu \wedge \omega \in \Omega^{N+1}(\mathbb{C}^{N+1})$, and therefore, for any holomorphic tangent vector $u \in T_p \mathbb{C}^{N+1}$, $u \neq 0$ is equivalent to $\iota_u(d_p \nu \wedge \omega_p) \neq 0$. This results in

$$\iota_v(d_p \nu \wedge \omega_p) = -d_p \nu \wedge \iota_v \omega_p + v^\nu \omega_p = v^\nu \omega_p \neq 0,$$

and thus $v^\nu \neq 0$.

By the holomorphic implicit function theorem, \mathcal{C} can be holomorphically parametrized by ν in a neighborhood of p . Together with $v^\lambda = 0$ it implies that we have $d\lambda/d\nu|_p = 0$ on \mathcal{C} . \square

Now, consider a smooth real curve parametrized by a real parameter t on the complex ν -plane that without degeneracy passes through 0. This curve is lifted to \mathcal{C} and the resulting smooth real curve is parametrized by t . From $d\lambda/d\nu = 0$ we conclude that $d\lambda/dt = 0$ at p too. In our case we have the curve $\mu(t) = e^{it}$ or $\nu(t) = e^{it} - 1$, which passes through $\mu = 1$ at $t = 0$. $\tilde{\mathcal{C}}$ is projected without degeneration to $\mathbb{C} \times \mathbb{R} \ni (\lambda, t)$ locally near p and then to $\mathbb{C} \ni \lambda$ with degeneration at the projection of p given by $d\lambda/dt = 0$.